Clays and Clay Minerals, Vol. 56, No. 2, 272–282, 2008.

QUANTITATIVE PHASE ANALYSIS OF BENTONITES BY THE RIETVELD METHOD

K. Ufer[1,*], H. Stanjek[2], G. Roth[3], R. Dohrmann[4], R. Kleeberg[5], and S. Kaufhold[4]

[1] TU Bergakademie Freiberg, Institute of Mineralogy, 09596 Freiberg, Germany
[2] Clay and Interface Mineralogy, RWTH Aachen University, 52056 Aachen, Germany
[3] Institute of Crystallography, RWTH Aachen University, 52056 Aachen, Germany
[4] BGR/LBEG, 30655 Hannover, Germany

Abstract—Thirty six bentonite samples from 16 different locations were examined in order to demonstrate the applicability of a new Rietveld description approach for quantitative phase analysis. X-ray diffraction patterns of the bulk material were obtained and analyzed by the Rietveld method. The samples contain up to ten different minerals, with dioctahedral smectite as the major component. A model for turbostratic disorder of smectites was formulated inside a structure-description file of the Rietveld program BGMN. The quality of the refinements was checked using an internal standard mineral (10.0 or 20.0 wt.% corundum) and by cross-checking results with X-ray fluorescence (XRF) data. The corundum content was reproduced with only small deviations from the nominal values. A comparison of the chemical composition obtained by XRF and the composition as re-calculated from quantitative Rietveld results shows a satisfactory agreement, although X-ray amorphous components such as volcanic glasses were not considered. As a result of this study, the Rietveld method combined with the new structure model for turbostratic disorder has proven to be a suitable method for routine quantitative analysis of bentonites with smectites as the dominant clay minerals.

Key Words—Bentonite, Quantification, Rietveld Analysis, Smectite.

INTRODUCTION

The quantitative mineral content of bentonites is important in applied studies as well as in geological interpretation. For this reason, a fast and accurate method for quantitative phase analysis (QPA) is desirable. Microscopic methods fail in the presence of clays. The lack of chemical contrast from coexisting silicates prevents the use of element analyses as the sole information for quantitative phase analysis as proposed, *e.g.* by Herrmann and Berry (2002). Several ways to determine smectite contents have been proposed and compared by Kahr (1998) and Kaufhold *et al*. (2002), based on smectite-specific properties such as cation exchange capacity or crystallite-size distribution. However, since powder X-ray diffraction (XRD) not only provides qualitative information on minerals in a powder but also allows for the determination of quantitative phase information, this method offers several ways to gain information on mineral-phase contents.

Traditional XRD methods for QPA are based on the determination of intensities of selected reflections and a comparison with reference intensities, either from internal or external reference phases (Snyder and Bish, 1989). For clay-dominated materials, size fractionation and preparation of highly oriented specimens for XRD is a widespread method (Moore and Reynolds, 1997), although this procedure mainly provides qualitative information. For the quantitative evaluation of patterns of these oriented slides, either single-line methods or computer-based simulation methods are used. All these methods are based on the assumption that the degree of orientation is identical for all minerals in the mixture or at least known for the case of different orientations on the slide. This presumption is not valid even for simple minerals such as illites (Reynolds, 1989), and consequently the technique of quantification from slides containing oriented material often fails. More recently, techniques based on randomly oriented samples have been introduced. The prerequisite is a random orientation of the particles, accomplished either by special techniques to fill the sample holder (*e.g.* Środoń *et al*., 2001; Zhang *et al*., 2003) or by preparation of spherical aggregates by spray drying (*e.g.* Hillier, 1999). However, the application of such techniques does not always guarantee full randomness, and the spray-drying procedure can produce some alteration of the minerals. Despite such limitations, different quantification methods have been developed to quantify clay minerals from random preparations. The most successful ones are based on full-pattern-fitting procedures (Omotoso *et al*., 2006). Their application requires extensive calibration and the collection of pure reference mineral patterns. Unfortunately, such a laborious procedure prohibits routine application to varying systems for a broader community of laboratories and less experienced researchers.

In recent years, the Rietveld method (Rietveld, 1967), which consists of an automatic, whole powder-pattern calculation and refinement of structural data against

* E-mail address of corresponding author:
kristian.ufer@bgr.de
DOI: 10.1346/CCMN.2008.0560210

observed data, opened the way towards a fast and accurate QPA method (Bish and Post, 1993). Unfortunately, clay minerals often show stacking faults and hence the description of clay particles as ideal crystallites which produce intensity only at distinctive Bragg peak positions is inappropriate. Therefore, different models were developed to handle disordered phases inside a Rietveld refinement. The most popular and successful approach was the introduction of 'observed *hkl* files' instead of a structure model (Taylor and Matulis, 1994). The procedure consists of the creation of a list of structure factors, based on an ideal structure model, but modified manually to fit the pattern of a disordered structure, such as that of montmorillonites. As a limitation, the structural parameters cannot be refined using this method. Nevertheless, the method is popular in practical phase quantification because it was implemented in the commercial software SIROQUANT™.

To handle structural disorder of clay minerals, several structure models for particular clay minerals were developed (Bergmann and Kleeberg, 1998). Such models are essentially based on an ideal structure model and an *hkl*-dependent line broadening and shifting according to the type of disorder. Smectites, in particular, which almost always show turbostratic disorder, could not be handled by the Rietveld method.

Turbostratic disorder can be regarded as a random rotation and/or translation of individual layers relative to each other (Warren, 1941; Biscoe and Warren, 1942). This kind of disorder leads to extremely broad and asymmetric non-basal reflections. Simulations of powder patterns from substances which show this kind of disorder can be performed by different approaches (Treacy *et al*., 1991; Drits and Tchoubar, 1990; Yang and Frindt, 1996) but the handling of turbostratic disorder inside a Rietveld refinement had not been possible before now. Several attempts were made to fit the reflections of turbostratically disordered smectites (Viani *et al.*, 2002), but the first structurally based method to simulate this kind of disorder was proposed by Ufer *et al*. (2004). The application of this new approach in a 'round-robin' test for QPA proved that it is capable of determining smectite contents accurately (Omotoso *et al*., 2006). In this study we show the applicability of this approach in determining the quantitative mineralogical composition of bentonites not only for the purpose (and under the conditions) of in-depth examinations but also in day-to-day laboratory routine.

MATERIALS AND METHODS

In order to prove the practicability of the new structure model for routine analysis, 36 bentonite samples from different localities were examined. These materials were derived directly from a deposit without any further processing (except for samples 24–27 which underwent industrial drying and grinding).

The samples were analyzed by XRD and XRF. In order to evaluate QPA with the new approach, only XRD data were considered for qualitative and quantitative analysis of the mineralogical composition. The results of the chemical analysis of the bulk material served merely as a cross check. As the only pre-treatment, the samples were ground in a McCrone mill (using agate grinding elements) before XRD and XRF measurements. An internal standard (20.0 wt.% corundum for samples 1–9 and 10.0 wt.% for samples 10–36) was added before the XRD measurements to evaluate the quality of the QPA.

As an additional test, the model was applied to an artificial mixture of a smectite-rich material. The <2 μm fractions of a Hungarian bentonite, quartz, calcite, and two feldspars were mixed. Before the XRD measurements 10.0 wt.% zincite was added as an internal standard.

Because of the strong dominance of smectites in the bentonites and their chemical variability, it was necessary during cross checking to determine the chemical composition of the smectites. Therefore, the <2 μm fraction of the bentonites was separated and analyzed by XRF. This fraction can be regarded as consisting mainly of smectite. The cation population which mainly stems from the interlayer was determined using the Cu-triethylenetetramine CEC method (Kahr and Meier, 1996). Mg occurs as an exchangeable cation and in the octahedral sheet of smectite. With the cation-exchange procedure, only the natural exchange population was desorbed, releasing exchangeable Na, K, Mg, and Ca. Octahedral Mg was not substituted by the index cation of the exchange solution. Roughly half of all samples are calcareous. Usually calcite is partially dissolved in such exchange experiments (Dohrmann, 2006) yielding erroneous exchangeable Ca values. As the bentonites were not $NaCO_3$-activated it was possible to correct the amount of exchangeable Ca by using the equation {Ca = CEC − (Mg+Na+K)}. The XRF results and the exchange population were then used to calculate the theoretical chemical composition. These formulae were also used for occupancies in the Rietveld structure model and for the calculation of a chemical composition for the cross check.

To estimate the influence of the individual chemical composition on the Rietveld refinement, two samples, one with the largest Fe content of the <2 μm fraction and another with the smallest Fe content in the same fraction, were recalculated with a mean smectite composition, considering the chemical composition of all 36 smectites in this study. The Fe should have the greatest impact due to greater atomic mass and number of electrons relative to Mg or Al.

XRF

The powdered samples were analyzed using a PANalytical Axios PW2400 spectrometer. Samples were prepared by mixing with a flux material and

https://doi.org/10.1346/CCMN.2008.0560210 Published online by Cambridge University Press

melting into glass beads. The beads were analyzed by wavelength-dispersive X-ray fluorescence spectrometry (WD-XRF). To determine the loss on ignition (LOI), 1.000 g of sample material was heated to 1030ºC for 10 min. After mixing the residue with 5.0 g of lithium metaborate and 25 mg of lithium bromide, it was fused at 1200ºC for 20 min. The calibrations were validated by the analysis of reference materials. 'Monitoring' samples and 130 certified reference materials (CRM) were used for the correction procedures.

XRD

The XRD patterns of the bentonites were recorded using a Philips X'Pert PW3710 θ–2θ diffractometer (CuKα radiation generated at 40 kV and 40 mA), equipped with a 1º divergence slit, 2.5º soller slits (primary and secondary), a 0.2 mm detector slit, a secondary monochromator, a point detector, and a sample changer (sample diameter 28 mm). The samples were measured from 2 to 80º2θ with a step size of 0.02º2θ and a measuring time of 3 s per step. For specimen preparation, a top-loading technique was used.

The artificial mixture was measured on an URD-6 (Seifert) diffractometer (Co radiation), equipped with a secondary beam graphite monochromator, proportional counter, a 0.2 mm detector slit, and an automatic divergence slit irradiating 15 mm sample length. Two measurements of the same sample were performed with the same diffractometer setting: (1) a 'routine' pattern with a 0.03º2θ step and 5 s counting time, total measuring time of ~125 min; and (2) a 'high-quality' pattern with 0.02º2θ step and 20 s counting time, total measuring time of ~1250 min. The measured interval was 5 to 80º2θ in both cases. The powder was inserted, by means of a side-loading technique, into a 27 mm diameter sample holder.

For the qualitative analysis of the bentonites, the software package Diffrac Plus (Bruker-AXS), combined with the powder diffraction file (PDF) database, was used. No additional information such as the chemical analysis was used for the identification.

Rietveld refinement and disorder model

The program BGMN was used for the Rietveld refinement (Bergmann *et al.*, 1998). BGMN uses a

Table 1. Results of the Rietveld quantification of 36 bentonite samples. The contents are given as wt.%; R_{wp} and R_{exp} as %.

Sample	1	2	3	4	5	6	7	8	9	10	11	12	13	14	15	16	17	18
R_{wp}	7.53	7.72	7.34	7.58	9.72	8.69	8.31	8.15	9.05	8.56	6.95	8.40	7.70	8.48	8.64	10.36	9.81	7.83
R_{exp}	5.23	5.40	5.46	5.69	5.72	5.37	5.38	5.57	5.50	5.77	5.99	5.72	5.79	5.70	6.05	5.27	4.82	5.12
Corundum	23.1	22.9	23.8	21.5	22.6	22.7	22.4	19.4	19.5	11.5	11.3	10.9	11.3	12.2	12.5	12.8	9.9	10.5
Smectite	77.6	76.6	89.6	91.6	89.1	93.2	91.7	62.7	58.8	89.6	89.2	91.0	86.8	87.6	70.3	57.8	95.2	92.3
Muscovite (1*M*)								1.8	3.0									
Muscovite ($2M_1$)		2.9														34.2	2.8	
Illite																		
Kaolinite													2.7	3.5	3.2	3.1		
Chlorite																		
Quartz	2.5	1.4	0.9	1.7	1.1		1.8	23.6	8.5	6.4	1.3	1.4	5.5	3.3	6.7	4.6	0.8	1.8
Cristobalite	0.3		1.9					1.1	11.4									
Hematite										0.6	0.1	2.4						
Ilmenite										0.8	0.1							
Rutile										0.7	0.3		0.2	0.4	0.5			
Anatase	0.4									1.4	2.5		1.4	2.0	1.3			
Goethite											5.6							
Calcite	0.9				5.4		1.3	0.9	8.0	0.6	0.8	0.9	2.9	0.5	15.7		0.5	0.8
Dolomite							1.0										0.8	
Siderite																		
Barite				1.5											0.4			
Gypsum				0.0	0.8			0.3	0.3							0.4		
Orthoclase	6.9		2.6	1.6	2.1	3.5	1.7	3.1	4.7									2.2
Sanidine		8.1																
Anorthite							2.6											
Albite	11.3		5.0	3.6		3.3		3.7	3.8									2.9
Plagioclase (An_{50})		11.2											0.6	2.8	1.9			
Heulandite								1.4	0.8									
Analcime								1.4	0.6									
Clinoptilolite																		
Pyrite					1.4													
Fluorapatite												4.3						

https://doi.org/10.1346/CCMN.2008.0560210 Published online by Cambridge University Press

fundamental parameter approach to model the peak profiles (Cheary and Coelho, 1992). For the predetermination of the instrument-dependent part of the diffraction profile a ray-tracing procedure was performed. This ray tracing is also used for beam-overflow corrections for intensities measured below 12°2θ.

BGMN is able to handle the model for the turbostratic disorder of smectites (Ufer *et al*., 2004). This model approximates the continuous intensity distribution of the reciprocal rods (resulting from the turbostratic stacking order) by a set of discrete but narrowly spaced Bragg peaks. This is attained by using a super cell which is obtained by elongating a standard cell in the *c* direction. To eliminate the periodicity in the *c* direction, this super cell is only filled to less than half of the cell volume. An *hkl*-dependent peak-broadening model smears the intensity between the distinct reciprocal positions to produce a smooth development of the diffraction line and to avoid the occurrence of ripples produced by the top part of the discrete peaks. This approach is able to model the asymmetric broad reflections of turbostratic disordered layer structures.

The atomic structure of the dioctahedral smectites was derived from models for dehydrated and K-saturated smectites by Tsipurski and Drits (1984). The interlayer space was increased to a basal distance of 12.5 Å to represent a mono-hydrated smectite and to 15 Å to represent a bi-hydrated smectite. In the case of the bi-hydrated smectite the interlayer cation is coordinated octahedrally by six water molecules and the octahedron is oriented in such a way that two triangles are aligned parallel to the layer surface. The cations in the mono-hydrated smectites are square-planar coordinated by water molecules oriented parallel to the TOT layers (unit of the two tetrahedral sheets and the octahedral sheet).

The cation occupancies in the octahedral sheet, the tetrahedral sheet, and the interlayer complexes were estimated from the XRF analysis of the <2 μm fraction and from CEC determination. These occupancies were kept fixed in the refinement. Before the refinement, the hydration state (mono-hydrated or bi-hydrated) was determined from the d_{001} value and the corresponding model was selected. Refined parameters of the smectite structure were the lattice parameters *a, b*, and *c*,

Table 1 (*contd*.)

Sample	19	20	21	22	23	24	25	26	27	28	29	30	31	32	33	34	35	36
R_{wp}	7.03	9.55	8.38	7.08	8.16	7.45	9.84	8.24	7.80	7.55	9.16	9.12	7.96	9.78	8.23	8.41	9.75	7.88
R_{exp}	5.18	5.15	5.03	4.87	4.97	4.99	5.32	4.84	5.11	4.98	5.35	5.47	5.78	5.43	6.00	5.94	5.45	5.77
Corundum	10.7	9.5	9.7	10.6	10.9	11.6	9.6	9.2	10.6	9.1	9.0	10.4	10.1	11.1	11.7	9.6	9.1	9.9
Smectite	76.4	85.7	80.3	76.0	79.9	81.3	43.2	83.0	74.7	69.0	87.4	80.6	92.4	88.3	77.0	75.1	80.4	63.0
Muscovite (1*M*)	4.0	1.8				3.7			3.0								5.5	
Muscovite ($2M_1$)							16.6											
Illite																		8.5
Kaolinite							21.9				5.2				1.3	2.2		
Chlorite																		0.3
Quartz	4.0	4.5	0.9	4.0	9.8	0.7	13.2	1.0	5.6	2.0	5.9	7.2	0.2	3.3	20.4	11.0	6.3	10.9
Cristobalite		1.7	1.3	11.7		2.2		12.4	7.8	8.0		8.7	0.1	0.9		3.3		0.2
Hematite																		
Ilmenite																		
Rutile																0.1		
Anatase											1.5	0.5			0.6			1.4
Goethite																		
Calcite	2.2	0.4		0.3				0.5	0.7			0.9					0.2	7.3
Dolomite													0.5					0.7
Siderite													0.2					
Barite						0.1												
Gypsum		0.6							0.2					0.2				
Orthoclase	3.3		5.5	3.4	3.2	6.5	1.7	3.1	3.9	2.3					0.7	6.3	4.4	
Sanidine																		
Anorthite									4.1									
Albite		5.4					3.5					1.2						
Plagioclase (50An)	10.1		12.1	4.7	7.1	6.2				2.1			1.9	7.3		2.0	3.3	7.7
Heulandite																		
Analcime																		
Clinoptilolite										16.7		1.0	4.6					
Pyrite																		
Fluorapatite																		

https://doi.org/10.1346/CCMN.2008.0560210 Published online by Cambridge University Press

anisotropic peak broadening, the cation distribution over the *cis*- and *trans*-octahedra position, and orientation parameters of the interlayer cation complex.

The structural data of the additional minerals were taken from the ICSD structure database (with minor changes). Structural parameters for the corundum standard were predetermined in a separate measurement and kept fixed during the quantification. For all minerals except smectite, only lattice parameters, peak-broadening parameters, and (if necessary) corrections for preferred orientation were refined with physically reasonable constraints.

As non-structural parameters, the zero point, the sample displacement error, and a Lagrange polynomial of 9th degree for background modeling were refined. Thus, up to 147 parameters (sample 9) had to be varied in such intricate samples. All refinements were performed by the full automatic BGMN algorithm without any user interaction or manual definition of a parameter-turn-on sequence. In that way, the procedure runs independently of user skill and is applicable to routine laboratory work.

Cross check of the quantitative results

Chemical analysis by XRF (Table 2) was chosen as an independent method for the assessment of the quantitative results obtained from the Rietveld refinement (Table 1). To compare the results of the two methods, a normative chemical composition was calculated from the relative amounts of the mineral phases determined by the Rietveld refinement. This procedure is an indirect method for evaluating the plausibility of *a priori* unknown phase compositions of complex systems (*e.g.* Monecke *et al*., 2001; Ward and Gómez-Fernández, 2003). To overcome the problem of high variability in smectite composition, the individual chemistry of the smectites was considered, estimated from the chemical composition of the <2 μm fraction.

Table 2. Chemical composition (wt.%, determined by XRF) of 36 bentonite samples.

Sample	SiO_2	TiO_2	Al_2O_3	Fe_2O_3	MnO	MgO	CaO	Na_2O	K_2O	LOI	Total
1	53.3	0.2	16.6	2.8	0.1	4.1	1.7	1.3	0.9	18.7	99.7
2	52.0	0.6	15.4	5.0	0.1	4.4	1.7	0.9	1.1	18.5	99.5
3	52.1	0.7	16.6	4.9	0.1	3.1	1.6	0.6	0.3	19.5	99.5
4	49.4	0.7	15.6	8.0	0.0	3.1	0.9	0.6	0.4	19.5	98.3
5	47.6	0.7	15.9	6.0	0.0	3.0	4.4	0.4	0.5	20.2	98.8
6	52.8	0.7	18.0	3.4	0.0	3.5	1.5	0.5	0.5	18.7	99.5
7	54.8	0.3	17.0	3.2	0.1	4.5	1.5	2.0	1.5	14.5	99.3
8	66.8	0.1	15.7	3.1	0.0	1.5	0.9	2.6	0.4	8.3	99.5
9	59.6	0.1	14.7	3.0	0.3	1.4	5.4	2.2	0.4	12.2	99.3
10	49.4	1.9	13.9	11.4	0.0	2.6	1.5	0.8	0.5	17.5	99.6
11	46.1	2.4	14.4	15.7	0.1	2.5	0.9	1.8	0.1	15.9	99.8
12	47.9	0.6	13.6	9.8	0.0	3.9	3.1	1.6	0.1	17.7	98.3
13	44.6	2.0	16.2	10.1	0.1	2.1	3.1	0.1	0.6	20.4	99.3
14	45.8	2.1	16.8	9.9	0.0	2.2	1.6	0.1	0.7	20.3	99.4
15	38.3	1.7	13.8	8.8	0.2	2.0	10.2	0.2	0.5	23.0	98.6
16	51.5	0.4	20.1	5.9	0.0	2.9	1.4	0.1	1.7	15.5	99.4
17	54.5	0.3	17.4	3.2	0.1	4.2	1.9	2.0	1.0	14.6	99.2
18	53.6	0.2	16.7	3.1	0.0	4.2	1.7	1.2	0.9	18.1	99.6
19	54.1	0.2	15.5	3.4	0.0	4.3	2.9	1.2	1.2	16.7	99.6
20	60.8	0.1	19.0	3.6	0.0	2.3	1.2	2.0	0.5	9.9	99.4
21	54.2	0.2	20.7	2.2	0.0	2.0	1.2	2.0	1.1	15.8	99.5
22	62.4	0.2	15.0	1.1	0.0	3.3	1.0	2.3	0.4	13.9	99.7
23	58.7	0.2	17.5	1.1	0.0	3.1	1.2	2.5	0.5	14.8	99.6
24	53.2	0.2	21.2	2.0	0.0	2.1	1.3	2.0	1.0	16.6	99.4
25	55.0	0.5	18.1	5.8	0.0	2.3	1.2	0.3	1.7	14.8	99.7
26	62.3	0.1	14.0	1.1	0.0	3.0	1.7	0.8	0.7	15.9	99.7
27	59.2	0.2	19.2	3.7	0.0	2.3	1.3	2.3	0.5	10.7	99.3
28	58.8	0.2	13.5	2.1	0.0	3.1	2.7	0.1	0.5	18.4	99.6
29	49.8	1.2	21.0	5.4	0.0	1.9	1.1	0.0	0.1	19.3	99.8
30	59.7	0.7	13.7	4.7	0.0	3.2	1.8	2.0	0.7	13.1	99.4
31	52.1	0.4	12.8	8.4	0.0	2.7	1.9	0.4	0.5	20.1	99.4
32	58.6	0.1	19.5	3.6	0.0	2.4	1.2	2.1	0.5	11.4	99.4
33	57.9	0.6	15.5	7.2	0.0	2.4	1.6	0.2	0.6	13.4	99.5
34	61.7	0.8	17.5	8.1	0.1	1.6	1.3	0.4	1.4	6.7	99.6
35	63.3	0.1	20.1	2.4	0.1	3.4	1.9	0.5	0.8	7.0	99.5
36	54.6	0.7	16.0	3.1	0.1	2.5	5.8	1.0	0.9	14.7	99.3

https://doi.org/10.1346/CCMN.2008.0560210 Published online by Cambridge University Press

A source of uncertainty is the *a priori* unknown chemical composition and amount of X-ray amorphous material in the bentonites. Even if it were possible to determine with the greatest precision the amount of X-ray amorphous material by the internal standard method as described below, the unknown chemical composition of the glass component would prohibit a complete and accurate recalculation of the sample chemistry. The limitations resulting from this problem in case of larger amounts of glass are discussed in the results section.

Another difficulty in the comparison of the calculated and observed chemical composition is the estimate of the amount of volatile components which are evolved before XRF measurements of the material. This can be divided into non-structural proportions, such as pore water, and structural proportions, such as OH^- in hydroxides or CO_3^{2-} in carbonates, which elute during heating. A differentiation between structural and non-structural components is difficult to calculate. Therefore, the loss on ignition in the pre-treatment for the XRF analysis was ignored. The XRD results contain only structural components. Proportions of non-structural components were not detectable. To correct for the influence of volatile structural components, the normative composition was only calculated from the oxide forms of the minerals.

Application to an artificial mixture

The patterns of the artificial mixture of smectite, quartz, calcite, and two feldspars were analyzed first, using starting structures which were not optimized to match the minerals of this mixture. In order to treat the material equally to the unknown bentonite samples, the two feldspars were modeled with the same structure models as the bentonite samples. For the plagioclase, a pure albite, and for the K feldspar, an orthoclase was chosen, ignoring the fact that not all peak positions are fitted properly. In a second refinement, the albite structure model was replaced by an oligoclase (plagioclase 16An) model, and the orthoclase by an adularia structure having structure parameters closer to the peak positions of the reference feldspars used in the mixture. The structural model for the smectite was calculated with the mean composition of the bentonites examined.

RESULTS AND DISCUSSION

Bentonite samples

Table 1 shows the mineralogical compositions of the 36 bentonites determined by the Rietveld refinement. The results are given without listing the compositions of the internal standard or the X-ray amorphous components. For better comparison, all values are specified with one decimal digit which certainly suggests a greater degree of accuracy than is actually achievable. The samples contain between three and ten different minerals. Smectite is always the most abundant component. Additional layer silicates are muscovite, illite, kaolinite, and chlorite. In most cases, these minerals were treated as ordered. Only in the case of kaolinite in sample 25 was a structure model with disorder parameters applied. Although naturally occurring feldspars show a high variability, only five models were considered in this work (two alkali feldspars and three plagioclases). The flexibility of the chosen models allows a description of a large range of different feldspars. Figures 1 and 2 show

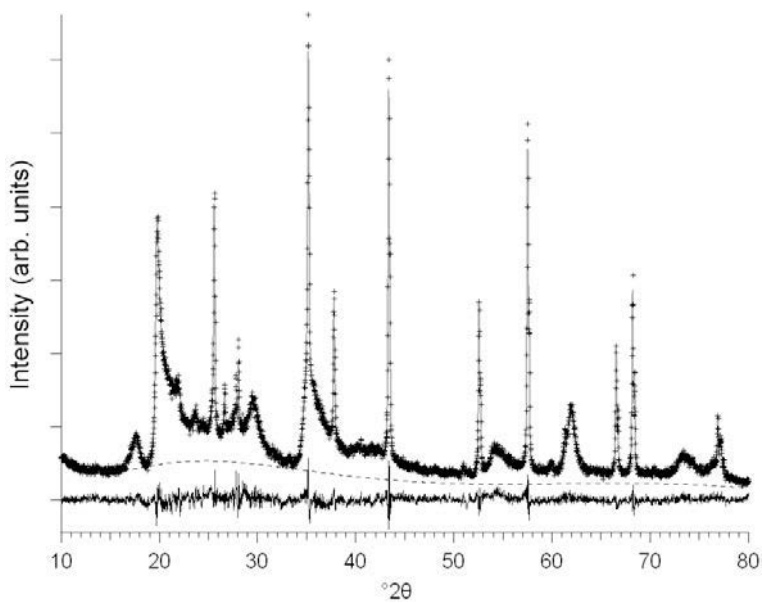

Figure 1. Rietveld plot of the refinement of sample 3. +: observed data. Gray line: calculated data. Dashed line: background. Continuous black line: difference curve.

https://doi.org/10.1346/CCMN.2008.0560210 Published online by Cambridge University Press

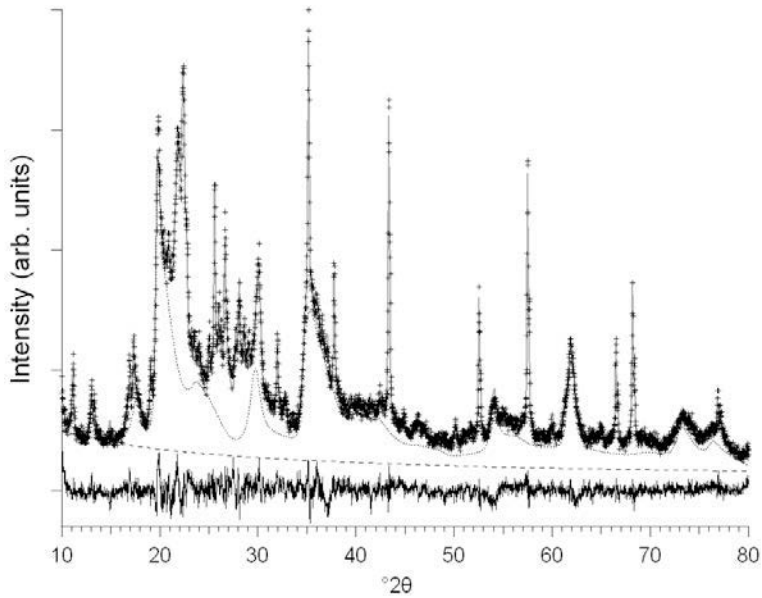

Figure 2. Rietveld plot of the refinement of sample 28. +: observed data. Gray line: calculated data. Dashed line: background. Continuous black line: difference curve. The dotted line represents the diffraction profile of the smectite.

two examples for the refinement results. Figure 1 shows the pattern of sample 3, a bentonite with high smectite content. This pattern is dominated by the smectite diffraction profile, which is also shown in the figure. The pattern shown in Figure 2 (sample 28) is covered by a large number of mainly clinoptilolite reflections.

The corundum standard contents could be recovered satisfactorily by all refinements, although a tendency towards higher values is obvious. These overestimations indicate the presence of additional X-ray amorphous components. This assumption is in some cases supported by the occurrence of an amorphous 'hump', as seen in Figure 1 in the 20–30º2θ region. The chemical composition of this X-ray amorphous phase is unknown. Therefore, only the crystalline components were considered for the cross check. This probably decreases the quality of the compliance of normative chemical composition and observed chemical composition as these X-ray amorphous components should differ in chemical composition from the average composition of the crystalline fraction of the bentonite.

The determination of the hydration state from the basal distance showed that almost all smectites show a non-rational series of basal reflections and the position of the 001 reflection lies between the expected values of approx. 12.5 Å for a mono-hydrated smectite and 15 Å for a bi-hydrated smectite with a certain tendency for one of the states. This can be interpreted as a mixed layering of both states and reflects the mixed exchange population of mono- and bivalent cations and inhomogeneous hydration states of these cations. Figure 3 shows this effect for sample 23. Thus far, it has proven impossible to handle this additional disordering and therefore the refinement was performed for data above 10º2θ with a *d* spacing suitable to fit the remaining 00*l* reflections. The error caused by this uncertainty is relatively small as most of the intensity of the powder pattern comes from non-basal reflections.

Figures 4 to 6 show the comparison of the chemical composition calculated from the Rietveld results and measured by XRF. In the case of exact agreement, the points would lie on the dashed line. Points below this line indicate an overestimation, and points above it, an underestimation by the Rietveld results.

For SiO_2 and Al_2O_3, all samples show good accord between values from XRD and XRF (Figure 4). The deviation from the ideal agreement for Fe_2O_3 and MgO (Figure 5) is larger than for SiO_2 and Al_2O_3, but both oxides follow the trend of the $y = x$ line. In most

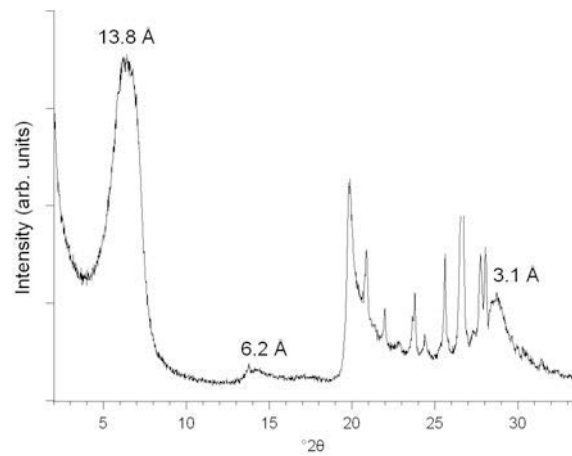

Figure 3. Powder XRD pattern of sample 23. The *d* values indicate a non-rational series of basal reflections.

https://doi.org/10.1346/CCMN.2008.0560210 Published online by Cambridge University Press

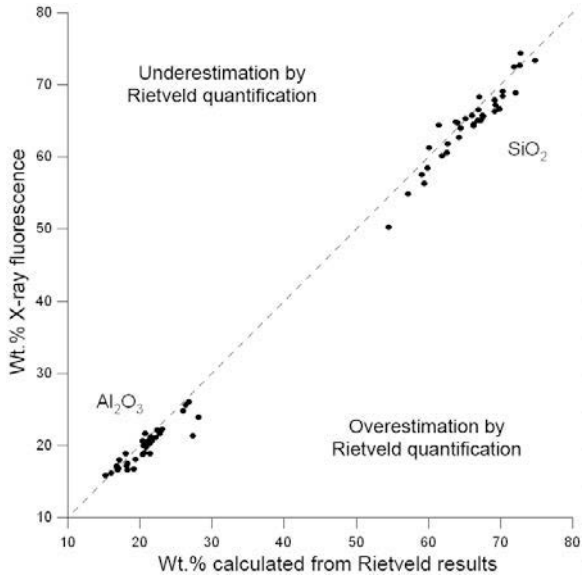

Figure 4. Comparison of the theoretical composition, calculated from the Rietveld quantification, with the chemical composition, from XRF, for the oxides of Si and Al.

samples, Mg and Fe were underestimated by the Rietveld results. The main carrier of Mg and Fe are the smectites. Only two samples contain chlorite, five contain dolomite, three pyrite, one siderite, and one goethite, these being the only Mg- and Fe-bearing minerals considered (except smectite). For most samples, Ti minerals were not identified. This leads to a strong underestimation by the Rietveld analysis. In order to improve the quantification, a loop back to the qualitative analysis would certainly be necessary. By identifying minor phases and including them in the Rietveld refinement, the misfit between chemical analysis and calculated chemical composition would be reduced.

The comparison of CaO, Na_2O, and K_2O shows a clear dispersion (Figure 6). The occurrence of these elements is related to the feldspars, and for Ca, is related also to the carbonates. The choice of only five different feldspars was not flexible enough to reflect the complex chemical composition of the minerals occurring. The remaining uncertainties are the X-ray amorphous components such as volcanic glasses.

To cross check all calculated chemical compositions against the measured compositions, it was necessary to consider the individual chemical compositions of the smectites. However, the determination of the smectite composition from the <2 μm fraction is a rough estimation, but it obviously improved the quality of the cross check. To estimate the impact of the individual smectite composition on the Rietveld refinement, two samples (sample 10 and 22) underwent additional refinement with a mean composition of the TOT structural unit. This mean composition, calculated from the composition of all 36 smectites, is $(Al_{1.40}Fe^{3+}_{0.30}Mg_{0.30})^{VI}(Si_{3.85}Al_{0.15})^{IV}O_{10}(OH)_2$. Sample 10 has the largest Fe content in the <2 μm fraction of all the bentonites examined. The TOT composition is $(Al_{1.10}Fe^{3+}_{0.65}Mg_{0.25})^{VI}(Si_{3.75}Al_{0.25})^{IV}O_{10}(OH)_2$. Sample 22, the bentonite with the smallest Fe content in the <2 μm fraction, has the composition $(Al_{1.49}Fe^{3+}_{0.07}Mg_{0.44})^{VI}(Si_{4.00}Al_{0.00})^{IV}O_{10}(OH)_2$. Table 3 compares the quantitative results of these two samples, calculated using the individual composition and using the mean composition.

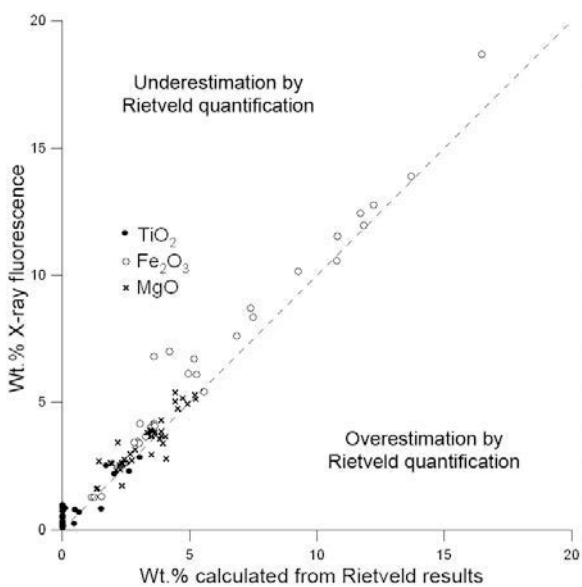

Figure 5. Comparison of the theoretical composition, calculated from the Rietveld quantification, with the chemical composition, from XRF, for the oxides of Ti, Fe, and Mg.

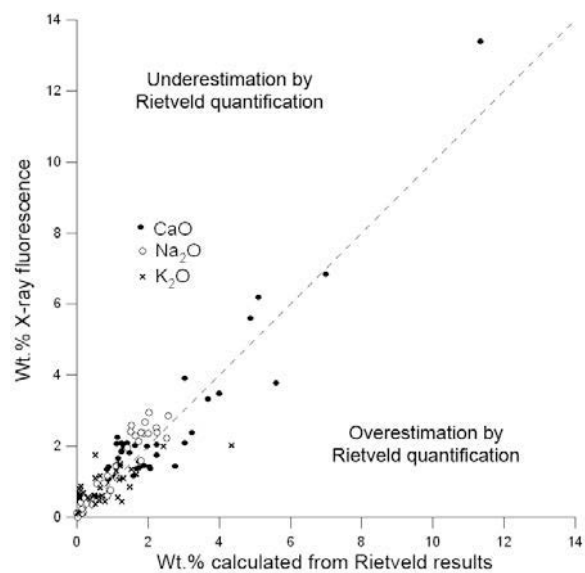

Figure 6. Comparison of the theoretical composition, calculated from the Rietveld quantification, with the chemical composition, from XRF, for the oxides of Ca, Na, and K.

https://doi.org/10.1346/CCMN.2008.0560210 Published online by Cambridge University Press

Table 3. Results of the Rietveld quantification of samples 10 and 22, calculated with the individual and with the mean smectite compositions. The contents are given as wt.%; R_{wp} and R_{exp} are given as %.

Sample	10	10 mean	10 bias	22	22 mean	22 bias
R_{wp}	8.56	8.62		7.08	7.20	
R_{exp}	5.77	5.77		4.87	4.86	
Corundum	11.5	11.0	0.5	10.6	10.6	0.0
Smectite	89.6	90.1	0.5	76.0	73.7	2.3
Quartz	6.4	6.1	0.3	4.0	4.2	0.2
Cristobalite				11.7	12.2	0.6
Hematite	0.6	0.4	0.2			
Ilmenite	0.8	0.7	0.1			
Rutile	0.7	0.6	0.1			
Anatase	1.4	1.4				
Calcite	0.6	0.7	0.1	0.3	0.3	0.0
Orthoclase				3.4	3.4	0.1
Plagioclase (An_{50})				4.7	6.1	1.5
Sum bias			1.3			4.7

For both samples the agreement criteria (R values and internal standard) are satisfactory, both if calculated using individual compositions as well as using mean compositions. For sample 10 the differences in mineralogical contents are quite small. For sample 22 the use of the mean composition led to a decrease in smectite content, compensated mainly by an increase in the plagioclase content.

ARTIFICIAL MIXTURE

The results of the simplified refinement and the second optimized refinement using additional information obtained from both measurements are shown in Table 4. From the overestimation of the internal standard, an X-ray amorphous content of 2.6–6.0 wt.% was calculated. It is assumed that the <2 μm fraction of the Hungarian bentonite used for the mixture contains some X-ray amorphous material, as indicated by previous investigations in preparation of the second Reynolds Cup contest (Kleeberg, 2004). In addition, small amounts of feldspars below the estimated XRD detection limit of 1–2 % may be also present in the <2 μm fraction of the bentonite. The total purity of the smectite can be estimated as 92–95 wt.%. Thus, the 'true' smectite content of the mixture is ~71–73 wt.%. The phase composition was calculated from the ratio of the weighted scale factors of the phases related to the internal standard zincite. The difference from 100% was assumed to be 'X-ray amorphous'. Within the BGMN program, the estimated standard deviation of all concentration values was calculated by error propagation from the refined parameters. The 3σ values are given in Table 4. Although the R_{wp} is more suited to the optimized refinement and for the high-quality measurement, respectively, there are no significant differences between the four results. Slight systematic underestimation of the calcite content and overestimation of the

Table 4. Results of the analysis of an artificial mixture. The contents are given as wt.%; R_{wp} and R_{exp} are given as %.

	Initial wt.%	Simplified composition calculated wt.% ±3σ		Optimized composition calculated wt.% ±3σ	
Measurement		0.03°, 3 s	0.02°, 20 s	0.03°, 3 s	0.02°, 20 s
R_{exp}		5.16	2.64	5.16	2.64
R_{wp}		7.07	5.43	6.75	4.79
Smectite	71–73*	72.8±2.7	71.3±1.9	73.3±2.7	71.4±1.9
Amorphous	4–6	4.5±3.3	6.0±2.1	2.6±3.3	4.2±2.1
Plagioclase	5	4.4±0.4	4.5±0.3	5.3±0.6	5.6±0.3
Alkali feldspar	5	5.3±0.6	5.4±0.5	6.0±0.6	6.0±0.5
Calcite	3	2.7±0.5	2.5±0.3	2.4±0.4	2.4±0.3
Quartz	10	10.2±0.4	10.3±0.3	10.3±0.4	10.4±0.3

* the true concentration is 71–73 wt.% because of X-ray amorphous material in the <2 μm fraction. The initial weight was 77 wt.% of the <2 μm fraction, containing significant amounts of X-ray amorphous material.

https://doi.org/10.1346/CCMN.2008.0560210 Published online by Cambridge University Press

K-feldspar seems to be independent of the models and of the data quality. As expected, the estimated standard deviations of the results from the routine measurement are greater than those from the high-quality measurement. In general, although it is necessary to make some assumptions to assess these results, it can be seen that even with imperfect qualitative composition, the smectite content can be determined accurately. On the other hand, the uncertainties in the determination of the X-ray amorphous content are relatively high and, consequently, a quantification of a small amount of X-ray amorphous material with large error seems to be of limited value for routine analysis.

CONCLUSIONS

The quantitative analysis of 36 bentonites showed that the Rietveld method combined with the new structure model is a suitable method for 'routine' quantitative analysis. The use of information exclusively from XRD led to reasonable values for phase contents. The additional examination of an artificial mixture demonstrated that, even with routine measurements, parameters, and non-optimized structure models, reliable values can be obtained. The individual chemical composition has only a small influence on the quantification. Even with an average smectite composition, satisfactory results can be achieved. However, knowledge of the individual chemical composition of the dominant smectites is necessary for a chemical cross check. This cross check is helpful in terms of improving the QPA, *e.g.* for a re-examination of the qualitative composition to discover minor components. There is further potential for the improvement of quantification, *e.g.* with more accurate examination of minerals with high variability such as feldspars. X-ray amorphous components can only be quantified indirectly by an internal standard and are still difficult to handle, because they influence the XRD characterization as well as the chemical-analysis methods in a complex way. In this work, however, we omitted further steps in order to show the capacity of the Rietveld method without supporting analyses.

The interstratification of different hydration states of the smectites is a serious draw-back. So far no structure model is capable of handling stacking disorder of layers with different spacings in a Rietveld refinement. A further development would be necessary. At present, only an extensive sample preparation and/or the control of measuring conditions may help to limit the problem of interstratification.

ACKNOWLEDGMENTS

The authors thank associate editor Bruno Lanson and the reviewers for their helpful suggestions which improved the manuscript.

REFERENCES

Bergmann, J. and Kleeberg, R. (1998) Rietveld analysis of disordered layer silicates. *Materials Science Forum*, **278–281**, 300–305.

Bergmann, J., Friedel, P., and Kleeberg, R. (1998) BGMN – a new fundamental parameter based Rietveld program for laboratory X-ray sources, its use in quantitative analysis and structure investigations. *Commission of Powder Diffraction. International Union of Crystallography, CPD Newsletter*, **20**, 5–8.

Biscoe, J. and Warren, B.E. (1942) An X-ray study of carbon black. *Journal of Applied Physics*, **13**, 364–371.

Bish, D.L. and Post, J.E. (1993) Quantitative mineralogical analysis using the Rietveld full-pattern fitting method. *American Mineralogist*, **78**, 932–940.

Cheary, R.W. and Coelho, A.A. (1992) A fundamental parameters approach to X-ray line-profile fitting. *Journal of Applied Crystallography* **25**, 109–121.

Dohrmann, R. (2006) Cation exchange capacity methodology I: An efficient model for the detection of incorrect cation exchange capacity and exchangeable cation results. *Applied Clay Science*, **34**, 31–37.

Drits, V.A. and Tchoubar, C. (1990) *X-ray Diffraction by Disordered Lamellar Structures*. Springer Verlag, New York, 371 pp.

Herrmann, W. and Berry, R.F. (2002) MINSQ – a least squares spreadsheet method for calculating mineral proportions from whole rock major element analyses. *Geochemistry: Exploration, Environment, Analysis*, **2**, 361–368.

Hillier, S. (1999) Use of an air-brush to spray dry samples for X-ray powder diffraction. *Clay Minerals*, **34**, 127–135.

Kahr, G. (1998) Methoden zur Bestimmung des Smektitgehaltes von Bentoniten. Pp. 163–172 in: *Berichte der DTTG* (K.-H. Henning and J. Kasbohm, editors). DTTG, Greifswald, Germany.

Kahr, G. and Meier, L.P. (1996) Einfache Bestimmungsmethode des Kationenaustauschvermögens von Tonen mit Komplexverbindungen des Kupfer(II)-Ions mit Triethylentetramin und Tetraethylenpentamin. Pp. 122–126 in: *Berichte der DTTG* (D. Wolf, R. Starke and R. Kleeberg, editors). DTTG, Freiberg, Germany.

Kaufhold, S., Dohrmann, R., Ufer, K., and Meyer, F.M. (2002) Comparison of methods for the quantification of montmorillonite in bentonites. *Applied Clay Science*, **22**, 145–151.

Kleeberg, R. (2004) Results of the second Reynolds Cup contest in quantitative mineral analysis. *Commission of Powder Diffraction, International Union of Crystallography CPD Newsletter*, **30**, 22–24.

Monecke, T., Köhler, S., Kleeberg, R., Herzig, P., and Gemmell, J.B. (2001) Quantitative phase-analysis by the Rietveld method using X-ray powder-diffraction data: Application to the study of alteration halos associated with volcanic-rock-hosted massive sulfide deposits. *The Canadian Mineralogist*, **39**, 1617–1633.

Moore, D.M. and Reynolds, R.C., Jr. (1997) *X-ray Diffraction and the Identification and Analysis of Clay Minerals*, 2nd edition. Oxford University Press, New York, 332 pp.

Omotoso, O., McCarty, D.K., Hillier, S., and Kleeberg, R. (2006) Some successful approaches to quantitative mineral analysis as revealed by the 3rd Reynolds contest. *Clays and Clay Minerals*, **54**, 748–760.

Reynolds, R.C. (1989) Principles and techniques of quantitative analysis of clay minerals by X-ray powder diffraction. Pp. 437 in: *Quantitative Mineral Analysis of Clays* (D.R. Pevear and F.A. Mumpton, editors). *CMS Workshop lectures*, **1**, The Clay Minerals Society, Boulder, Colorado, USA.

Rietveld, H.M. (1967) Line profiles of neutron powder-

diffraction peaks for structure refinement. *Acta Crystallographica*, **22**, 151–152.

Snyder, R.L. and Bish, D.L. (1989) Quantitative analysis. Pp. 101–144 in: *Modern Powder Diffraction* (D.J. Bish and J.E. Post, editors). Reviews in Mineralogy, **20**, Mineralogical Society of America, Washington, D.C.

Środoń, J., Drits, V.A., McCarty, D.K., Hsieh, J.C.C., and Eberl, D.D. (2001) Quantitative X-ray diffraction analysis of clay-bearing rocks from random preparations. *Clays and Clay Minerals*, **49**, 514–528.

Taylor, J.C. and Matulis, C.E. (1994) A new method for Rietveld clay analysis. Part I. Use of a universal measured standard profile for Rietveld quantification of montmorillonites. *Powder Diffraction*, **9**, 119–123.

Treacy, M.M.J., Newsam, J.M., and Deem, M.W. (1991) A general recursion method for calculating diffracted intensities from crystals containing planar faults. *Proceedings of the Royal Society, London*, **A433**, 499–520.

Tsipursky, S.I. and Drits, V.A. (1984) The distribution of octahedral cations in the 2:1 layers of dioctahedral smectites studied by oblique texture electron diffraction. *Clay Minerals*, **19**, 177–192.

Ufer, K., Roth, G., Kleeberg, R., Stanjek, H., Dohrmann, R. and Bergmann, J. (2004) Description of X-ray powder pattern of turbostratically disordered layer structures with a Rietveld compatible approach. *Zeitschrift für Kristallographie*, **219**, 519–527.

Viani, A., Gualtieri, A.F., and Artioli, G. (2002) The nature of disorder in montmorillonite by simulation of X-ray powder patterns. *American Mineralogist*, **87**, 966–975.

Ward, C.R. and Gómez-Fernández, F. (2003) Quantitative mineralogical analysis of Spanish roofing slates using the Rietveld method and X-ray powder diffraction data. *European Journal of Mineralogy*, **15**, 1051–1062.

Warren, B.E. (1941) X-ray diffraction in random layer lattices. *Physical Reviews*, **59**, 693–698.

Yang, D. and Frindt, R.F. (1996) Powder X-ray diffraction of turbostratically stacked layer systems. *Journal of Materials Research*, **11**, 1733–1738.

Zhang, G., Germaine, J.T., Martin, R.T., and Whittle, A.J. (2003) A simple sample-mounting method for random powder X-ray diffraction. *Clays and Clay Minerals*, **51**, 218–225.

(*Received 24 April 2007; revised 22 January 2008; Ms. 0024; A.E. B. Lanson*)